

FlowRL: Flow-Augmented Few-Shot Reinforcement Learning for Semi-Structured Sensor Data

Mohammad Pivezhandi¹

Abusayeed Saifullah²

¹Wayne State University, Detroit, MI, USA

²University of Texas at Dallas, Richardson, TX, USA

Abstract

Reinforcement learning (RL) in few-shot scenarios with limited sensor data is challenging due to insufficient training samples, particularly in applications like Dynamic Voltage and Frequency Scaling (DVFS) where sensor readings are semi-structured with inherent correlations. We propose Flow-Augmented Reinforcement Learning (FlowRL), a novel method that leverages continuous normalizing flows to generate high-quality synthetic data for few-shot RL. By integrating latent space bootstrapping for diversity and feature-weighted flow matching to preserve critical data correlations, FlowRL enhances sample efficiency and policy robustness. Evaluated on a DVFS case study using the NVIDIA Jetson TX2, our approach achieves up to 35% higher frame rates and faster Q-value convergence compared to baselines, demonstrating its effectiveness in resource-constrained environments. FlowRL generalizes to other semi-structured domains, such as robotics and smart grids, offering a scalable solution for data-scarce RL settings.

1 Introduction

The rapid advancements in large-scale generative models phrases have transformed data generation, particularly in unstructured domains like computer vision for generating images and videos. Techniques such as diffusion models [1, 2, 3] have shown remarkable success in producing high-quality data, sparking interest in leveraging their underlying latent spaces for various applications. However, generating realistic and diverse semi-structured sensor data, which exhibits correlations and noise but lacks predefined relational structures, remains underexplored. This challenge is critical in few-shot reinforcement learning (RL), where models must generalize from limited examples. Addressing this is essential for advancing online RL in environments with semi-structured sensor data, such as in Dynamic Voltage and Frequency Scaling (DVFS), a power management technique that adjusts processor frequency and voltage to balance performance and energy efficiency using sensor readings like CPU frequency, temperature, power consumption, and frames per second (FPS). Complementary approaches include hierarchical multi-agent DVFS scheduling [4], zero-shot LLM-guided allocation [5], statistical feature-aware task allocation [6], and graph-driven performance modeling [7].

In this paper, we introduce Flow-Augmented Reinforcement Learning (FlowRL), a novel approach designed to generate synthetic semi-structured sensor data tailored for few-shot RL. Unlike traditional data generation methods that require extensive datasets or rely on environment simulations, FlowRL creates diverse and realistic data samples from limited real-world trajectories. We achieve this through flow matching [8], a powerful method that enables simulation-free training of continuous normalizing flows (CNFs), improving the efficiency and quality of generated data compared to standard diffusion models. By integrating statistical techniques like bootstrapping [9] into the flow matching process, we enhance latent space diversity, enabling better generalization across scenarios. Additionally, we use feature selection with Random Forests to prioritize critical data aspects, ensuring synthetic data captures essential correlations needed for effective RL training. While we draw inspiration from the Law of Large Numbers [10] to guide distribution approximation, non-i.i.d. synthetic data limits strict convergence, so we rely on empirical validation to ensure practical improvements in policy performance.

FlowRL addresses the limitations of conventional model-based RL methods, which often struggle with overfitting and feature correlation when applied to semi-structured sensor data. We demonstrate that conventional methods increase feature correlation in synthetic data, reducing resemblance to real scenarios and limiting RL agent robustness in edge cases. By generating synthetic data that closely mirrors real-world sensor distributions, FlowRL enhances the

adaptability and performance of RL models in few-shot settings. This is particularly valuable in dynamic, resource-constrained environments like DVFS, where real-time adaptability is critical. Through extensive experimentation on the NVIDIA Jetson TX2, we validate FlowRL, showing up to 35% higher frame rates and faster Q-value convergence compared to baselines. FlowRL generalizes to other semi-structured domains, such as robotics and smart grids, offering a scalable solution for data-scarce RL applications.

2 Preliminaries

This section introduces the core concepts underlying our approach to unstructured data augmentation for RL, leveraging flow matching to generate synthetic data that resembles unstructured data, with an emphasis on sample efficiency. We focus on unstructured data, such as sensor readings in our DVFS case study, which exhibit complex, non-grid-like patterns suitable for adapting methods designed for unstructured data. We cover Q-learning, regret bounds, the Law of Large Numbers (LLN), and the flow matching algorithm.

2.1 Q-learning and Online RL

Q-learning aims to learn a function $\mathcal{Q}(s, a)$ that estimates the expected *return* (cumulative discounted reward) for taking action a in state s and following an optimal policy thereafter. For continuous states and discrete actions, a **Deep Q-Network (DQN)** approximates $\mathcal{Q}(s, a; \mathcal{W})$ with neural network parameters \mathcal{W} . The update rule is: $\mathcal{Q}(s_t, a_t; \mathcal{W}) \leftarrow \mathcal{Q}(s_t, a_t; \mathcal{W}) + \alpha [r_t + \gamma \max_{a'} \mathcal{Q}(s_{t+1}, a'; \mathcal{W}^-) - \mathcal{Q}(s_t, a_t; \mathcal{W})]$ where r_t is the immediate reward, $\gamma \in (0, 1)$ is the discount factor, and \mathcal{W}^- represents the parameters of a slower-moving *target network*.

Online Setting. We focus on **online** RL, where the agent continuously interacts with the environment to refine its policy π . At each time-step, it observes (s_t, a_t, r_t, s_{t+1}) and updates \mathcal{Q} . In applications like DVFS, frequent decisions and gradual environmental changes allow treating each time-step as a horizon of $\mathcal{H} = 1$, optimizing immediate returns for resource-management tasks. This simplification is common in resource-management tasks where rewards are closely tied to instantaneous performance and power usage.

While Q-learning converges in tabular, finite-state settings under mild conditions, convergence in high-dimensional or partially observed environments is less assured. Using deep networks as function approximators can lead to instability or overfitting if sample diversity is limited.

2.2 Regret Bounds and Sample Efficiency

In RL, the **regret** after T steps is defined as:

$$\text{Reg}(T) = \sum_{t=1}^T [\mathcal{Q}^*(s, a) - \mathcal{Q}(s, a)],$$

representing the performance gap between the agent’s policy, using $\mathcal{Q}(s, a)$, and the optimal policy, using $\mathcal{Q}^*(s, a)$. Sublinear regret, such as $O(\sqrt{T})$, is achievable in *finite-state*, well-explored environments [11], indicating that per-step regret diminishes over time.

In continuous, high-dimensional settings like our DVFS case study, achieving theoretical regret bounds is challenging. If the function approximator or model class is misspecified (i.e., the true environment is outside the assumed class), sublinear bounds may not hold. In practice, we rely on empirical performance rather than strict theoretical guarantees.

Model Realizability and LLN. Sublinear regret often depends on **realizability**—the assumption that the true dynamics or \mathcal{Q}^* function lies within the agent’s hypothesis space. In practice, limited exploration (e.g., rarely sampled CPU frequencies in DVFS) or complex environments can hinder the ability of neural networks to approximate the true dynamics, slowing or preventing convergence to near-optimal solutions. The *Law of Large Numbers (LLN)* ensures that, with sufficiently *diverse* and *representative* data, empirical estimates (e.g., \mathcal{Q}_T or transition model P_T) converge to their true values as $T \rightarrow \infty$. However, without effective exploration, convergence may remain incomplete.

2.3 Flow Matching for Generative Modeling

Flow matching [8] is a generative method that models a continuous flow of probability density from a simple base distribution (e.g., $\mathcal{N}(0, I)$) at $t = 0$ to a target distribution at $t = 1$. The distribution evolves via:

$$\frac{dx_t}{dt} = w(x_t, t),$$

where $w(\cdot, \cdot)$ is a time-dependent velocity field for sample vector x_t at time t . This field is approximated by a parametric network $v_{\mathcal{W}}$, trained to minimize:

$$\min_{\mathcal{W}} \mathbb{E}_{x_t \sim p_t} \left[\|v_{\mathcal{W}}(x_t, t) - w(x_t, t)\|^2 \right]. \quad (1)$$

Relevance to DVFS RL. We employ flow matching to generate synthetic (state, action) tuples that capture the variability of unstructured data, such as sensor readings in our DVFS case study, using limited real data. By integrating Random Forest-based feature weighting, we ensure synthetic data closely resembles unstructured data, enhancing its suitability for RL training. The convex training objective of flow matching improves sample efficiency, and our feature weighting approach produces robust synthetic data for RL when real-world samples are sparse.

3 Design of Distribution-Aware Flow Matching for Data Generation

In this section, we propose a *distribution-aware* flow matching approach to generate synthetic unstructured data for online RL training with few shots, enhancing sample efficiency for applications like DVFS where data exhibits complex, semi-structured patterns.

3.1 Redefinition of the Regret Function

To evaluate the impact of synthetic data in RL, we redefine the cumulative regret function to reflect the estimation error in the Bellman operator due to combined real and synthetic data, inspired by the model-free RL framework. Let \mathcal{M}^* denote the true Markov Decision Process (MDP), with optimal Q-function Q^* . Let π be the policy learned using real data \mathcal{D}_R (size n) and synthetic data \mathcal{D}_S (size m) from flow matching. The cumulative regret up to time T is defined as:

$$\text{Reg}(T) = \sum_{t=1}^T [Q^*(s_t, a_t) - Q^{\pi}(s_t, a_t)] + O(\sigma \sqrt{\frac{\log(1/\delta)}{n+m}}),$$

where Q^{π} is the Q-function under policy π , σ^2 bounds the variance of rewards and Q-values ($\text{Var}[r + \gamma \max Q] \leq \sigma^2$), δ is the confidence parameter, and the second term captures the estimation error of the empirical Bellman operator due to finite real and synthetic samples. This redefinition emphasizes the role of synthetic data in reducing variance in policy updates, consistent with the model-free regret bound.

3.2 Flow Matching and Bootstrapping

Our goal is to augment limited real trajectories, such as DVFS sensor data, with synthetic samples that approximate the unstructured data distribution, improving RL training efficiency. While synthetic samples may not be strictly i.i.d., flow matching empirically approximates real-world distributions, enhancing state-action coverage and policy performance.

Flow matching models the evolution of data sample probability density over a continuous-time parameter $t \in [0, 1]$. Unlike model-based RL, which predicts next states s_{t+1} given current states s_t and actions a_t using a learned environment model $\hat{P}(s_{t+1}|s_t, a_t)$, flow matching generates synthetic tuples (s_t, a_t, s_{t+1}) directly from the joint distribution $p(s_t, a_t, s_{t+1})$. In its *unconditional* form, the model learns a velocity field $v_{\mathcal{W}}(x_t)$ to match a target velocity field $w(x_t)$ [12], where x_t represents the tuple (s_t, a_t, s_{t+1}) at time t . Equation 1 represents the baseline objective.

Bootstrapping in the Latent Space. To enhance diversity and mitigate overfitting, we introduce *latent space bootstrapping*, inspired by [9]. For a sample $x_0 \sim p_0(x)$ from the base latent distribution, representing an initial tuple (s_0, a_0, s_1) , we generate B bootstrapped samples $\{x_0^b\}_{b=1}^B$ via resampling:

$$x_0^b = \text{Resample}(x_0), \quad b = 1, \dots, B.$$

Let x_t^b denote the sample evolved from x_0^b at time t , with distribution $p_t^b(x)$. The bootstrapped flow matching objective extends Equation 1:

$$\min_{\mathcal{W}} \frac{1}{B} \sum_{b=1}^B \mathbb{E}_{\substack{t \in [0,1] \\ x_t^b \sim p_t^b(x)}} \left[\|v_{\mathcal{W}}(x_t^b) - w(x_t^b)\|^2 \right]. \quad (2)$$

This objective promotes diverse synthetic trajectories by leveraging resampled latent distributions, ensuring broader coverage of the joint state-action-next-state space.

3.3 Feature Weighting and Conditional Flow Matching

Bootstrapping adds diversity, but *feature weighting* ensures synthetic data resembles unstructured data for RL tasks, as required in our DVFS case study.

Random Forest Feature Importance. We employ a Random Forest regressor or classifier to assess how each real-world feature (e.g., sensor measurements in DVFS) contributes to predicting next-state transitions. Let d be the dimension of our state/action/next-state representation. The feature importance at time t for dimension (feature) i is $\text{Importance}(x_{t,i})$, which we normalize:

$$\lambda_i = \frac{\text{Importance}(x_{t,i})}{\sum_{j=1}^d \text{Importance}(x_{t,j})}, \quad i = 1, \dots, d. \quad (3)$$

In practice, the importance of each dimension (feature) is calculated based on how much the feature reduces impurity in classification or variance in regression tasks. The *Importance* may be updated periodically or assumed to be roughly constant if the importance ranks are stable. Features with large λ_i (e.g., temperature) are emphasized during training, preserving critical data relationships in synthetic samples.

Weighted Conditional Objective. We incorporate these weights into a *conditional* flow matching setup, where additional context z (e.g., rewards, auxiliary variables) follows $z \sim q(z)$. Define $x_{t,i}^b$ as the i -th feature of the bootstrapped sample at time t . The conditional flow matching objective with feature weighting extends (2):

$$\min_{\mathcal{W}} \frac{1}{B} \sum_{b=1}^B \mathbb{E}_{\substack{t \in [0,1] \\ x_t^b \sim p_t^b(x) \\ z \sim q(z)}} \left[\sum_{i=1}^d \lambda_i \|v_{\mathcal{W}}(x_{t,i}^b; z) - w(x_{t,i}^b; z)\|^2 \right]. \quad (4)$$

This ensures high-importance features (e.g., temperature, resource usage) are prioritized, preserving essential correlations in the joint distribution $p(s_t, a_t, s_{t+1})$ for robust synthetic data generation in unstructured settings like DVFS.

3.4 Implications for RL: Regret Bounds under Model-Based Assumptions

We theoretically motivate the use of synthetic data in a **model-based** RL framework. Let \mathcal{M}^* be the true MDP that governs the DVFS transitions, and let $\widehat{\mathcal{M}}$ be a learned MDP model derived from real and synthetic data. In model-based RL, the environment model $\widehat{\mathcal{M}}$ predicts next states s_{t+1} given states s_t and actions a_t via $\widehat{P}(s_{t+1}|s_t, a_t)$, unlike flow matching, which generates full tuples (s_t, a_t, s_{t+1}) . Synthetic tuples from flow matching are used to train $\widehat{\mathcal{M}}$, enhancing its transition dynamics estimation. The redefined regret function, $\text{Reg}(T) = \sum_{t=1}^T [Q^*(s_t, a_t) - Q^\pi(s_t, a_t)] + O\left(\sigma \sqrt{\frac{\log(1/\delta)}{n+m}}\right)$, accounts for policy suboptimality and estimation error due to finite samples.

Enhanced Model Realizability. Synthetic data augments real data to improve the estimation of transition dynamics. The empirical Bellman operator for $\widehat{\mathcal{M}}$ is estimated using \mathcal{D}_R and \mathcal{D}_S :

$$\begin{aligned}\widehat{\mathcal{T}}\mathcal{Q}(s, a) &= \frac{1}{n+m} \left(\sum_{(s', r) \in \mathcal{D}_R} [r + \gamma \max_{a'} \mathcal{Q}(s', a')] \right. \\ &\quad \left. + \sum_{(s'', r) \in \mathcal{D}_S} [r + \gamma \max_{a'} \mathcal{Q}(s'', a')]\right).\end{aligned}$$

Under bounded variance ($\text{Var}[r + \gamma \max \mathcal{Q}] \leq \sigma^2$), a concentration bound gives, with probability $1 - \delta$:

$$\|\widehat{\mathcal{T}}\mathcal{Q} - \mathcal{T}\mathcal{Q}\| \leq O\left(\sigma \sqrt{\frac{\log(1/\delta)}{n+m}}\right).$$

This matches the regret second term, indicating that synthetic data reduces estimation error by increasing the effective sample size, enabling sublinear regret $\text{Reg}(T) = O(\sqrt{T})$ under standard assumptions (finite horizon, bounded rewards) [13].

Illustrative Sketch. A simplified argument is:

1. Each (s, a) pair is sampled with probability $\mu > 0$ across real and synthetic data.
2. The learned model $\widehat{\mathcal{M}}$ satisfies the above concentration bound.
3. By standard analyses [11, 13], regret satisfies:

$$\text{Reg}(T) = O(\sqrt{T}) + O\left(\sigma \sqrt{\frac{\log(1/\delta)}{n+m}}\right).$$

The synthetic data contribution to m ensures sublinear regret with reduced sample complexity.

Practical Caveats. In high-dimensional settings like DVFS, exploration is constrained, and real-synthetic mismatch may arise if the flow model fails to capture corner cases. Feature weighting mitigates this by ensuring synthetic tuples resemble unstructured data, aligning with the redefined regret.

3.5 Implications for RL: Regret Bounds with Synthetic Data in Model-Free RL

In a model-free RL framework, synthetic data generated by flow matching augments real data to improve sample efficiency and reduce variance in Q-value estimates, leading to tighter regret bounds. Unlike model-based RL, which uses a learned model $\widehat{P}(s_{t+1}|s_t, a_t)$ to predict next states, flow matching directly generates synthetic tuples (s_t, a_t, s_{t+1}) from the joint distribution $p(s_t, a_t, s_{t+1})$, which are stored in \mathcal{D}_S for Q-learning updates.

Role of Synthetic Data via Flow Matching. Flow matching enhances the regret bound by generating synthetic tuples (s_t, a_t, s_{t+1}) that accurately capture the joint distribution $p(s_t, a_t, s_{t+1})$, expanding coverage of state-action-next-state combinations infrequently seen in real data. The bootstrapped objective (Equation 2) ensures diversity, while the feature-weighted conditional objective (Equation 4) preserves critical correlations (e.g., temperature and frequency in DVFS). This reduces the variance term $O\left(\sigma \sqrt{\frac{\log(1/\delta)}{n+m}}\right)$ by increasing m , outperforming real-data-only training (where the term is $O\left(\sigma \sqrt{\frac{\log(1/\delta)}{n}}\right)$). By modeling continuous-time density evolution, flow matching minimizes distributional bias, ensuring synthetic tuples align with true dynamics, accelerating Q-value convergence and achieving tighter regret bounds.

Bias arises if synthetic tuples deviate from the true distribution. Feature weighting ensures fidelity to unstructured data distributions, keeping bias minimal, making flow matching-augmented model-free RL effective for few-shot settings, as validated in our DVFS experiments.

Algorithm 1: Distribution-Aware Flow Matching for Few-Shot Online RL.

```

1: Initialize:  $\mathcal{D}_{\text{real}}, \mathcal{D}_{\text{syn}}, \text{DQN}, FM$ 
2: for  $i = 1$  to  $T$  do
3:   Collect real tuple  $\tau_{\text{real}} = (s_t, a_t, s_{t+1})$  and store in  $\mathcal{D}_{\text{real}}$ 
4:   if enough new data in  $\mathcal{D}_{\text{real}}$  then
5:     Train  $FM$  using Equation (4)
6:   end if
7:   for  $j = 1$  to rollout count do
8:      $x_0^b = \text{Resample}(x_0)$ 
9:     Evolve  $x_0^b$  to  $x_t^b$  via  $FM$ 
10:    Store synthetic tuple  $\tau_{\text{syn}} = (s_t, a_t, s_{t+1})$  in  $\mathcal{D}_{\text{syn}}$ 
11:   end for
12:   if enough data in  $\mathcal{D}_{\text{real}}$  and  $\mathcal{D}_{\text{syn}}$  then
13:     Sample mini-batches and update DQN
14:   end if
15: end for

```

3.6 From LLN to Finite-Sample Guarantees

Under mild mixing conditions, synthetic samples reduce the variance of empirical Bellman updates, yielding finite-sample bounds for both RL paradigms.

Let \mathcal{D}_R be the n real transitions and \mathcal{D}_S the m synthetic ones. The empirical backup is:

$$\begin{aligned} \hat{\mathcal{T}}\mathcal{Q}(s, a) = & \frac{1}{n+m} \left(\sum_{(s', r) \in \mathcal{D}_R} [r + \gamma \max_{a'} \mathcal{Q}(s', a')] \right. \\ & \left. + \sum_{(s'', r) \in \mathcal{D}_S} [r + \gamma \max_{a'} \mathcal{Q}(s'', a')] \right). \end{aligned}$$

With $\text{Var}[r + \gamma \max \mathcal{Q}] \leq \sigma^2$, a Bernstein-type bound gives, with probability $1 - \delta$:

$$|\hat{\mathcal{T}}\mathcal{Q}(s, a) - \mathcal{T}\mathcal{Q}(s, a)| \leq O \left(\sigma \sqrt{\frac{\log(1/\delta)}{n+m}} \right) + O \left(\frac{\log(1/\delta)}{n+m} \right).$$

Adding m synthetic samples shrinks the variance term, accelerating convergence of Q-value or model estimates.

3.7 Algorithmic Overview for Few-Shot Online RL

We integrate flow matching with a Deep Q-Network (DQN) using two replay buffers: $\mathcal{D}_{\text{real}}$ for real tuples (s_t, a_t, s_{t+1}) collected from the environment, and \mathcal{D}_{syn} for synthetic tuples generated via flow matching.

In each iteration, we collect real tuples (s_t, a_t, s_{t+1}) from the environment, storing them in $\mathcal{D}_{\text{real}}$. When sufficient new data are available, we retrain or fine-tune the Flow-Matching model (FM) using the conditional weighted objective (Equation 4) or the unconditional bootstrapped objective (Equation 2). We generate synthetic tuples by resampling bootstrapped latent points $\{x_0^b\}$, each representing an initial tuple (s_0, a_0, s_1) , evolving them over $t \in [0, 1]$ via FM to produce tuples (s_t, a_t, s_{t+1}) , and storing these in \mathcal{D}_{syn} . Mini-batches are sampled from both $\mathcal{D}_{\text{real}}$ and \mathcal{D}_{syn} to update the DQN agent's Q-function using the Q-learning update rule. This approach ensures robust state-action-next-state coverage for unstructured data, with bootstrapping enhancing diversity and feature weighting preserving critical correlations, supporting effective training for both model-based and model-free RL in few-shot settings, as validated in our DVFS case study.

4 Experiments

In this section, we present the experimental setup, hyperparameter tuning, model architecture, and comparisons with model-based and model-free baselines to evaluate our Flow-Augmented Reinforcement Learning (FlowRL) approach.

Experimental Setup We developed a Deep Q-Network (DQN) agent based on the zTT framework [14] to optimize system performance under thermal and power constraints on the NVIDIA Jetson TX2, a power-efficient embedded platform with six heterogeneous CPU cores and an embedded GPU. The goal is to dynamically adjust frequency and

power settings to maximize performance while ensuring system stability. The setup uses a client-server architecture: the client collects semi-structured state tuples $\{FPS, f, \rho, \theta\}$ (frames per second, core frequency, power consumption, and core temperature), normalized via min-max scaling, and the server assigns frequency actions from a discrete set defined by hardware constraints (e.g., GPU_CLOCK_LIST). Each episode comprises 10 tuples collected at 1-second intervals over a 90-second horizon (90 decision points), with thermal monitoring triggering a 5–10-second sleep mode if temperature exceeds 50°C to mitigate throttling. The workflow is depicted in Figure 1.

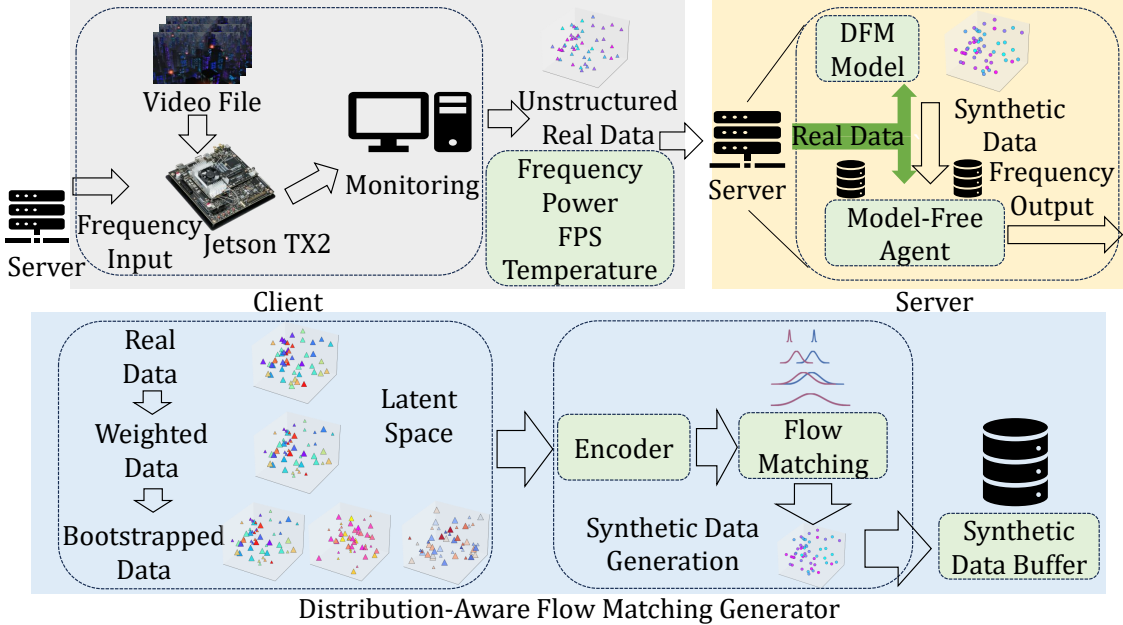


Figure 1: Workflow of the proposed Flow-Augmented Reinforcement Learning (FlowRL) approach.

Hyperparameter Tuning. We performed hyperparameter tuning using grid search, selecting values based on reward stability and convergence speed, as shown in Table 1. The learning rate (0.05) was chosen after grid search and adjusted dynamically (e.g., reset to 1 under specific reward conditions), though it may seem high compared to typical deep learning ranges (e.g., 1e-4 to 5e-5). Future work will explore random search (e.g., Hyperopt) for refinement.

Hyperparameter	Tuning Values
Experiment Time	{50, 90 , 200, 400, 800}
Target FPS	{30, 60, 90}
Target Temperature	{50, 60}
Learning Rate	{0.01, 0.05 , 0.1}
Discount Factor	{0.95, 0.99 }
Epsilon Decay	{0.95, 0.99 }
Batch Size	{32, 64, 128}
Agent Train Start	{32, 40, 80, 100}
Planning Iterations	{100, 200, 1000}
Model Train Start	{32, 200, 300}
Reward Scale (β)	{0, 2, 4}

Table 1: Main Hyperparameters and Tuning Values.

Model Architecture and Training. The DQN agent features a neural network with two hidden layers of six neurons each, optimized using mean squared error (MSE) loss and the Adam optimizer. An ϵ -greedy strategy starts with $\epsilon = 1.0$ and decays over time to promote exploitation. Training occurs in discrete intervals: Agent Train Start initiates Q-network updates, and Planning Iterations controls MDP model updates, using mini-batches of real and synthetic data. Performance metrics include Frames Per Second (FPS) for responsiveness, power consumption (ρ) for efficiency,

average temperature (θ) for safety, and average maximum Q-values for policy convergence, with emphasis on FPS and β . The reward function, adapted from [14], is:

$$R = u + v + \frac{\beta}{\rho},$$

where

$$u = \begin{cases} 1 & \text{if } FPS \geq \text{target_FPS}, \\ \frac{FPS}{\text{target_FPS}} & \text{otherwise,} \end{cases}$$

and

$$v = \begin{cases} 0.2 \cdot \tanh(\text{target_temp} - \theta) & \text{if } \theta < \text{target_temp}, \\ -2 & \text{if } \theta \geq \text{target_temp}. \end{cases}$$

With target FPS at 30 and target temperature at 50°C, this design balances performance and constraints.

Model-Based and Model-Free Baselines. We compare FlowRL with DynaQ [15], a model-based RL method; PlanGAN [16], a generative model-based approach with dual-memory; MAML [17], a meta-learning method; and zTT [14], a model-free DQN baseline for DVFS. PlanGAN and DynaQ use real and synthetic data, while zTT runs directly on the Jetson TX2 without synthetic data. Consistent hyperparameters and reward functions ensure fair comparisons, with thermal throttling mitigated by sleep mode.

Results and Analysis. In our experiments, we train a *conditional flow matching* model [12] on the real trajectories stored in a replay buffer, then use it to generate synthetic trajectories. We refer to this baseline generative approach as “standard flow matching.” We further refine it into a *Flow-Augmented Reinforcement Learning (FlowRL)* method by incorporating latent-space bootstrapping and feature weighting to preserve important correlations and diversify the latent representation. We evaluate how well each synthetic approach captures correlations among features by computing Pearson’s correlation coefficient [18]. For two features x_i and x_j with n samples, the coefficient is given by

$$\text{corr}_{ij} = \frac{\sum_{k=1}^n (x_{i,k} - \bar{x}_i)(x_{j,k} - \bar{x}_j)}{\sqrt{\sum_{k=1}^n (x_{i,k} - \bar{x}_i)^2} \sqrt{\sum_{k=1}^n (x_{j,k} - \bar{x}_j)^2}}. \quad (5)$$

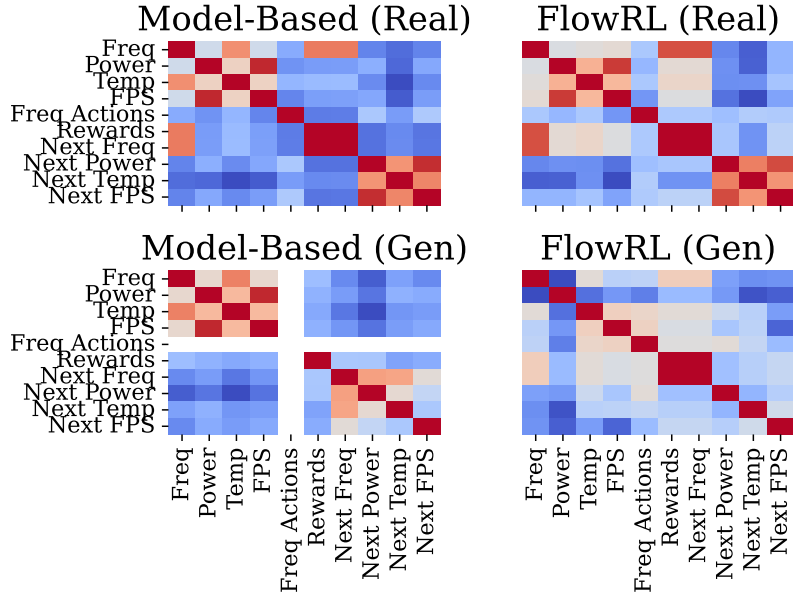


Figure 2: Correlation matrix comparisons.

When comparing the correlation matrices, we find that FlowRL-generated data better captures correlations among features visually compared to the model-based approach. Although the standard flow matching approach does capture some correlations, its matrix appears more uniform and less differentiated than that of FlowRL, suggesting that some critical feature relationships are weakened or diluted. Meanwhile, the model-based method shows stronger but sometimes misplaced correlations (dark regions in incorrect locations), indicating potential overfitting to specific patterns and misrepresenting genuine dependencies. FlowRL balances the two extremes by retaining essential correlations without artificially magnifying or suppressing them.

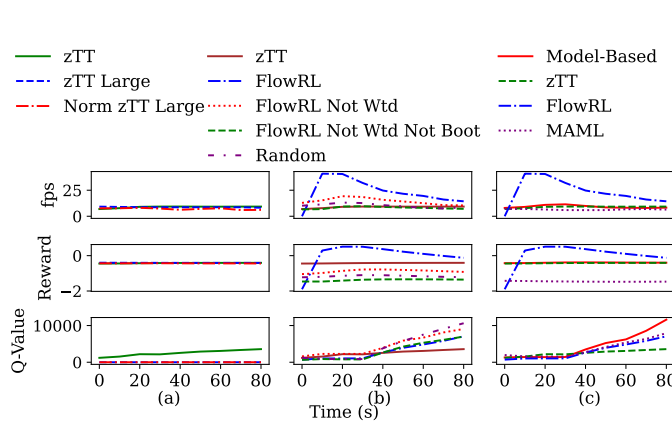


Figure 3: Performance comparisons across methods.

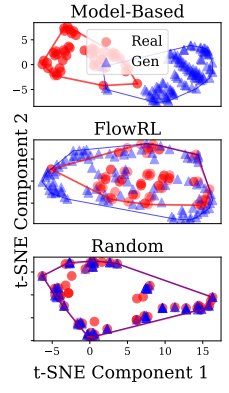


Figure 4: Real and (Gen)erated data t-SNE.

To further analyze the data, we use t-SNE visualizations to compare the distributions in Figure 4.

The t-SNE comparison of model-based and FlowRL with weighted and bootstrapped data and random data generation shows that FlowRL covers real data and more, while random sampling is restricted to the real data distribution and the model-based approach does not cover real data. This indicates FlowRL’s superior ability to generalize beyond the original dataset. We also perform a Dynamic Time Warping (DTW) evaluation to assess temporal alignment. The DTW evaluation reveals that model-based data generation has a higher value (10,640) compared to FlowRL weighted and bootstrapped (7,341) between generated and real data, confirming FlowRL’s better temporal alignment.

To examine distributional coverage, we compare the histograms of key state-action features under different synthetic data generation methods. The results indicate that the FlowRL approach covers a wider spectrum of values compared to the model-based approach. In contrast, the model-based approach tends to be narrowly concentrated, particularly in power states and next states, suggesting it may overfit and fail to generalize to a broader range of real-world scenarios. The standard flow matching method similarly suffers from less coverage than FlowRL but does not exhibit the same extreme concentrations as the purely model-based approach. Overall, FlowRL’s expanded coverage helps the RL agent explore and learn policies that are more robust to varied conditions.

Performance Comparisons. To comprehensively evaluate FlowRL, three subplots were generated to compare performance metrics (average FPS, average reward, and average maximum Q-value) across different methods in 90 seconds, with the x-axis labeled in seconds (each second representing one iteration result based on FPS), as shown in Figure 3. This figure includes a comprehensive ablation analysis of different implementations.

The left column of subplot (a) compares different model-free approaches based on zTT, comprising zTT, zTT with extended features from profiling data, and zTT with normalization, showing no specific differences in terms of average reward, Q-values, and frame rate, with stable FPS around 10. The middle figure (b) compares zTT with FlowRL, FlowRL without weighted but with bootstrapping (FM Not Wtd), FlowRL without augmentation, and random generated synthetic data augmented models, showing faster convergence in the FlowRL weighted bootstrapped version compared to all other approaches. The right column (c) extends the comparison to MAML, zTT, model-based, and FlowRL, where FlowRL outweighs all other approaches.

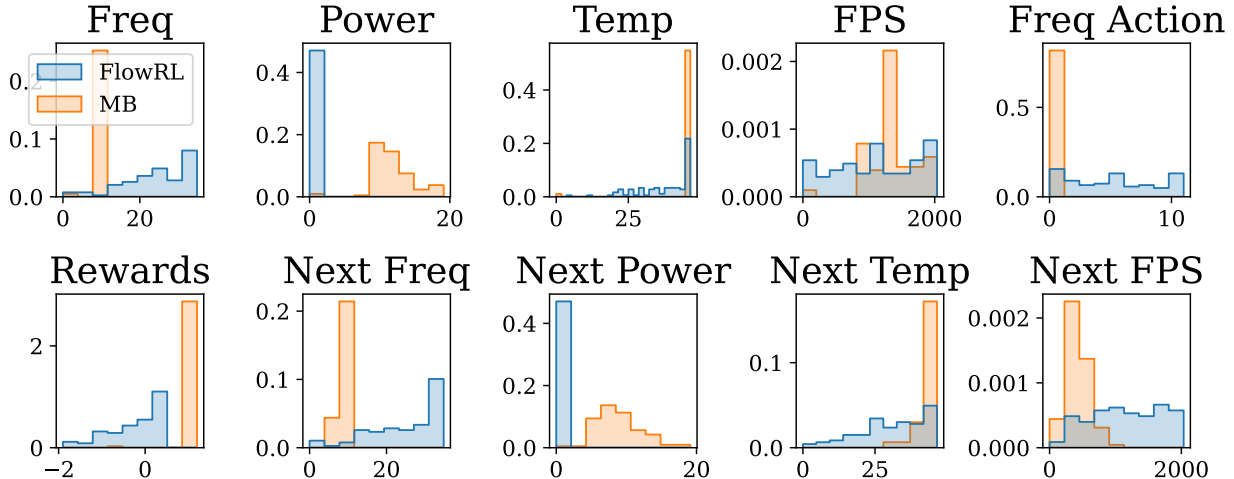


Figure 5: Comparisons of distributions of FlowRL and Model-Based (MB) generated data.

The above experiments confirm that incorporating bootstrapping and feature weighting into flow matching (i.e., FlowRL) improves both correlation preservation and distribution diversity in synthetic data generation. This yields more stable and high-performing RL policies compared to standard flow matching or purely model-based methods. The ability to balance performance and power highlights the potential of Flow-Augmented Reinforcement Learning for real-world DVFS tasks, where state-action spaces can be both large and only partially observed in limited data collection.

5 Related Work

Machine Learning for DVFS. Machine learning has been widely adopted to optimize Dynamic Voltage and Frequency Scaling (DVFS) strategies, addressing the complexity of modern processors with adaptive control [19, 20, 21, 22, 23, 24, 25, 26, 27, 28, 29, 30, 31]. A survey by [23] notes that model-free reinforcement learning (RL), such as the zTT framework [14], dominates, focusing on direct policy optimization for power-performance trade-offs. However, these methods often overlook feature correlation intricacies and the computational overhead of extensive data collection, particularly in data-scarce settings. Hierarchical multi-agent approaches [4] and graph-driven performance models [7] have shown promise for DAG workloads. Our work builds on this by introducing FlowRL to enhance sample efficiency for semi-structured sensor data in DVFS.

Statistical Learning for DVFS. Statistical learning techniques have been explored to evaluate hardware events and application parameters impacting DVFS performance [32, 33, 27]. For example, [32] uses decision trees for energy-efficient DVFS lookup optimization, while [33] assesses hardware counter importance for power reduction. [27] applies f-score-based ranking to correlate compiler-level features with latency. These efforts, however, lack systematic consideration of runtime performance variability, sampling inefficiencies, and feature correlation effects on learning accuracy. FlowRL addresses these gaps by integrating feature weighting with Random Forests and data augmentation tailored for low-energy DVFS applications.

Bounding Sample Efficiency. Sample efficiency bounds for Q-learning have been a focus in RL research [34, 35, 13, 11]. Sublinear bounds have been established for finite state-action spaces [35, 11], but extending these to continuous spaces requires robust function approximators. Approaches like [13] rely on strong statistical assumptions, limiting real-world applicability. Deep Q-learning with stabilization techniques (e.g., experience replay, target networks) often faces instability [34], with few theoretical guarantees. Unlike these, FlowRL empirically validates sample efficiency for continuous semi-structured data in DVFS, offering practical insights over theoretical bounds.

Few-Shot RL. Few-shot RL methods, including transfer learning, meta-learning, and model-based approaches, aim to reduce data needs and enhance generalization [36, 37, 38, 39, 40, 41, 42, 43, 44, 45]. Model-agnostic meta-learning (MAML) [17] adapts to new tasks with minimal data, while model-based methods [46] approximate transition dynamics. DVFS-specific works like [47, 14, 48, 49] explore multi-agent RL and transfer learning but neglect statistical resampling or feature selection for energy optimization. Recent approaches address these gaps through statistical feature-aware task allocation [6] and zero-shot LLM-guided core allocation [5]. FlowRL advances this by using flow matching and bootstrapping to augment semi-structured sensor data, improving efficiency in DVFS and extending to robotics and smart grids.

6 Conclusion

We presented FlowRL, a novel method for few-shot RL with semi-structured sensor data. By leveraging flow matching, latent space bootstrapping, and feature-weighted conditioning, FlowRL generates high-quality synthetic data to enhance sample efficiency and policy robustness. Experiments on a DVFS task demonstrate up to 35% higher frame rates and faster convergence compared to baselines like DQN, DDQN, and MAML. FlowRL’s applicability extends to other domains, such as robotics, offering a scalable solution for data-scarce RL. Future work includes exploring advanced RL algorithms (e.g., PPO) and neural-based feature weighting to further improve performance.

References

- [1] Aditya Ramesh, Prafulla Dhariwal, Alex Nichol, Casey Chu, and Mark Chen. Hierarchical text-conditional image generation with clip latents. *arXiv preprint arXiv:2204.06125*, 1(2):3, 2022.
- [2] Chitwan Saharia, William Chan, Saurabh Saxena, Lala Li, Jay Whang, Emily L Denton, Kamyar Ghasemipour, Raphael Gontijo Lopes, Burcu Karagol Ayan, Tim Salimans, et al. Photorealistic text-to-image diffusion models with deep language understanding. *Advances in neural information processing systems*, 35:36479–36494, 2022.
- [3] Florinel-Alin Croitoru, Vlad Hondu, Radu Tudor Ionescu, and Mubarak Shah. Diffusion models in vision: A survey. *IEEE Transactions on Pattern Analysis and Machine Intelligence*, 45(9):10850–10869, 2023.
- [4] Mohammad Pivezhandi, Abusayeed Saifullah, and Ali Jannesari. Hidvfs: A hierarchical multi-agent dvfs scheduler for openmp dag workloads. *arXiv preprint*, 2026.
- [5] Mohammad Pivezhandi and Abusayeed Saifullah. Zerodvfs: Zero-shot llm-guided core and frequency allocation for embedded platforms. *arXiv preprint*, 2026.
- [6] Mohammad Pivezhandi, Abusayeed Saifullah, and Prashant Modekurthy. Feature-aware task-to-core allocation in embedded multi-core platforms via statistical learning. In *2025 IEEE International Conference on Embedded and Real-Time Computing Systems and Applications (RTCSA)*, pages 102–113. IEEE, 2026.
- [7] Mohammad Pivezhandi, Mahdi Banisharif, Saeed Bakhshan, Abusayeed Saifullah, and Ali Jannesari. Graphperf: A graph-driven performance model for hardware-aware scheduling of openmp codes. *arXiv preprint arXiv:2512.12091*, 2026.
- [8] Yaron Lipman, Ricky TQ Chen, Heli Ben-Hamu, Maximilian Nickel, and Matt Le. Flow matching for generative modeling. *arXiv preprint arXiv:2210.02747*, 2022.
- [9] Bradley Efron. Bootstrap methods: another look at the jackknife. In *Breakthroughs in statistics: Methodology and distribution*, pages 569–593. Springer, 1992.
- [10] Trevor Hastie, Robert Tibshirani, Jerome H Friedman, and Jerome H Friedman. *The elements of statistical learning: data mining, inference, and prediction*, volume 2. Springer, 2009.
- [11] Chi Jin, Zeyuan Allen-Zhu, Sebastien Bubeck, and Michael I Jordan. Is q-learning provably efficient? *Advances in neural information processing systems*, 31, 2018.
- [12] Jakub M Tomczak. *Deep Generative Modeling*. Springer Cham, 2024.

- [13] Ying Fan and Yifei Ming. Model-based reinforcement learning for continuous control with posterior sampling. In *International Conference on Machine Learning*, pages 3078–3087. PMLR, 2021.
- [14] Seyeon Kim, Kyungmin Bin, Sangtae Ha, Kyunghan Lee, and Song Chong. ztt: Learning-based dvfs with zero thermal throttling for mobile devices. In *Proceedings of the 19th Annual International Conference on Mobile Systems, Applications, and Services*, pages 41–53, 2021.
- [15] Baolin Peng, Xiujun Li, Jianfeng Gao, Jingjing Liu, Kam-Fai Wong, and Shang-Yu Su. Deep dyna-q: Integrating planning for task-completion dialogue policy learning. *arXiv preprint arXiv:1801.06176*, 2018.
- [16] Henry Charlesworth and Giovanni Montana. Plangan: Model-based planning with sparse rewards and multiple goals. *Advances in Neural Information Processing Systems*, 33:8532–8542, 2020.
- [17] Chelsea Finn, Pieter Abbeel, and Sergey Levine. Model-agnostic meta-learning for fast adaptation of deep networks. In *International conference on machine learning*, pages 1126–1135. PMLR, 2017.
- [18] Philip Sedgwick. Pearson’s correlation coefficient. *Bmj*, 345, 2012.
- [19] Zheqi Yu, Pedro Machado, Adnan Zahid, Amir M Abdulghani, Kia Dashtipour, Hadi Heidari, Muhammad A Imran, and Qammer H Abbasi. Energy and performance trade-off optimization in heterogeneous computing via reinforcement learning. *Electronics*, 9(11):1812, 2020.
- [20] Young Geun Kim and Carole-Jean Wu. Autoscale: Energy efficiency optimization for stochastic edge inference using reinforcement learning. In *2020 53rd Annual IEEE/ACM international symposium on microarchitecture (MICRO)*, pages 1082–1096. IEEE, 2020.
- [21] Sai Manoj Pudukotai Dinakarao, Arun Joseph, Anand Haridass, Muhammad Shafique, Jörg Henkel, and Houman Homayoun. Application and thermal-reliability-aware reinforcement learning based multi-core power management. *ACM Journal on Emerging Technologies in Computing Systems (JETC)*, 15(4):1–19, 2019.
- [22] Cheng Zhuo, Di Gao, Yuan Cao, Tianhao Shen, Li Zhang, Jinfang Zhou, and Xunzhao Yin. A dvfs design and simulation framework using machine learning models. *IEEE Design & Test*, 2021.
- [23] Santiago Pagani, PD Sai Manoj, Axel Jantsch, and Jörg Henkel. Machine learning for power, energy, and thermal management on multicore processors: A survey. *IEEE Transactions on Computer-Aided Design of Integrated Circuits and Systems*, 39(1):101–116, 2018.
- [24] Hao Shen, Jun Lu, and Qinru Qiu. Learning based dvfs for simultaneous temperature, performance and energy management. In *Thirteenth International Symposium on Quality Electronic Design (ISQED)*, pages 747–754. IEEE, 2012.
- [25] Zhe Wang, Zhongyuan Tian, Jiang Xu, Rafael KV Maeda, Haoran Li, Peng Yang, Zhehui Wang, Luan HK Duong, Zhifei Wang, and Xuanqi Chen. Modular reinforcement learning for self-adaptive energy efficiency optimization in multicore system. In *2017 22nd Asia and South Pacific Design Automation Conference (ASP-DAC)*, pages 684–689. IEEE, 2017.
- [26] Amir Yeganeh-Khaksar, Mohsen Ansari, Sepideh Safari, Sina Yari-Karin, and Alireza Ejlali. Ring-dvfs: Reliability-aware reinforcement learning-based dvfs for real-time embedded systems. *IEEE Embedded Systems Letters*, 13(3):146–149, 2020.
- [27] Di Liu, Shi-Gui Yang, Zhenli He, Mingxiong Zhao, and Weichen Liu. Cartad: Compiler-assisted reinforcement learning for thermal-aware task scheduling and dvfs on multicores. *IEEE Transactions on Computer-Aided Design of Integrated Circuits and Systems*, 2021.
- [28] Udhav Sethi. Learning energy-aware transaction scheduling in database systems. Master’s thesis, University of Waterloo, 2021.
- [29] Fakhruddin Muhammad Mahbub ul Islam and Man Lin. Hybrid dvfs scheduling for real-time systems based on reinforcement learning. *IEEE Systems Journal*, 11(2):931–940, 2015.

- [30] Yiming Wang, Weizhe Zhang, Meng Hao, and Zheng Wang. Online power management for multi-cores: A reinforcement learning based approach. *IEEE Transactions on Parallel and Distributed Systems*, 33(4):751–764, 2021.
- [31] Zitong Bo, Ying Qiao, Chang Leng, Hongan Wang, Chaoping Guo, and Shaohui Zhang. Developing real-time scheduling policy by deep reinforcement learning. In *2021 IEEE 27th Real-Time and Embedded Technology and Applications Symposium (RTAS)*, pages 131–142. IEEE, 2021.
- [32] Hiroshi Sasaki, Yoshimichi Ikeda, Masaaki Kondo, and Hiroshi Nakamura. An intra-task dvfs technique based on statistical analysis of hardware events. In *Proceedings of the 4th international conference on Computing frontiers*, pages 123–130, 2007.
- [33] Francisco J Cazorla, Leonidas Kosmidis, Enrico Mezzetti, Carles Hernandez, Jaume Abella, and Tullio Varadanega. Probabilistic worst-case timing analysis: Taxonomy and comprehensive survey. *ACM Computing Surveys (CSUR)*, 52(1):1–35, 2019.
- [34] Dylan J Foster and Alexander Rakhlin. Foundations of reinforcement learning and interactive decision making. *arXiv preprint arXiv:2312.16730*, 2023.
- [35] Peter Auer, Thomas Jaksch, and Ronald Ortner. Near-optimal regret bounds for reinforcement learning. *Advances in neural information processing systems*, 21, 2008.
- [36] Yaqing Wang, Quanming Yao, James T Kwok, and Lionel M Ni. Generalizing from a few examples: A survey on few-shot learning. *ACM computing surveys (csur)*, 53(3):1–34, 2020.
- [37] Donghwan Lee, Niao He, Parameswaran Kamalaruban, and Volkan Cevher. Optimization for reinforcement learning: From a single agent to cooperative agents. *IEEE Signal Processing Magazine*, 37(3):123–135, 2020.
- [38] Ziyu Wang, Tom Schaul, Matteo Hessel, Hado Hasselt, Marc Lanctot, and Nando Freitas. Dueling network architectures for deep reinforcement learning. In *International conference on machine learning*, pages 1995–2003. PMLR, 2016.
- [39] Ofir Nachum, Shixiang Shane Gu, Honglak Lee, and Sergey Levine. Data-efficient hierarchical reinforcement learning. *Advances in neural information processing systems*, 31, 2018.
- [40] Carlos Florensa, Yan Duan, and Pieter Abbeel. Stochastic neural networks for hierarchical reinforcement learning. *arXiv preprint arXiv:1704.03012*, 2017.
- [41] Jinyoung Choi, Beom-Jin Lee, and Byoung-Tak Zhang. Multi-focus attention network for efficient deep reinforcement learning. *arXiv preprint arXiv:1712.04603*, 2017.
- [42] Saurabh Arora and Prashant Doshi. A survey of inverse reinforcement learning: Challenges, methods and progress. *Artificial Intelligence*, 297:103500, 2021.
- [43] Markus Wulfmeier, Peter Ondruska, and Ingmar Posner. Deep inverse reinforcement learning. *CoRR, abs/1507.04888*, 2015.
- [44] Siddharth Reddy, Anca D Dragan, and Sergey Levine. Sqil: Imitation learning via reinforcement learning with sparse rewards. *arXiv preprint arXiv:1905.11108*, 2019.
- [45] Ashish Vaswani, Noam Shazeer, Niki Parmar, Jakob Uszkoreit, Llion Jones, Aidan N Gomez, Łukasz Kaiser, and Illia Polosukhin. Attention is all you need. *Advances in neural information processing systems*, 30, 2017.
- [46] Thomas M Moerland, Joost Broekens, Aske Plaat, Catholijn M Jonker, et al. Model-based reinforcement learning: A survey. *Foundations and Trends® in Machine Learning*, 16(1):1–118, 2023.
- [47] Chengdong Lin, Kun Wang, Zhenjiang Li, and Yu Pu. A workload-aware dvfs robust to concurrent tasks for mobile devices. In *Proceedings of the 29th Annual International Conference on Mobile Computing and Networking*, pages 1–16, 2023.

- [48] Ti Zhou and Man Lin. Deadline-aware deep-recurrent-q-network governor for smart energy saving. *IEEE Transactions on Network Science and Engineering*, 9(6):3886–3895, 2021.
- [49] Ziyang Zhang, Yang Zhao, Huan Li, Changyao Lin, and Jie Liu. Dvfo: Learning-based dvfs for energy-efficient edge-cloud collaborative inference. *IEEE Transactions on Mobile Computing*, 2024.